



Radiographic and computed tomographic evaluation of vertebral injuries in dogs

Venkatesh V^{1*}, Vijayakumar M², Kathirvel S³ and Balasundaram K⁴.

¹PG scholar, ²Assistant Professor, ³Professor and Head, Department of Veterinary Surgery and Radiology,

⁴Professor and Head, Department of Veterinary Anatomy, Veterinary College and Research Institute, Namakkal-637002, Tamilnadu, India.

Corresponding Author: Venkatesh V^{1}

ABSTRACT: Spinal diseases in dogs are usually associated with some neurologic dysfunctions like paresis or paraplegia and more common in thoracolumbar spinal segment. Survey radiography and myelography are the commonly used for the diagnosis of spinal diseases but with poor diagnostic efficiency. Computed tomographic (CT) is an emerging important diagnostic tool, especially in canine orthopaedic cases and provide advantage over radiographs. The present study was conducted to evaluate the radiographical and computed tomographical findings in dogs with spinal injuries. Plain radiographic examination and computed tomography scan were performed in dogs with spinal injuries. Survey radiograph provided only the anatomical landmark whereas CT evaluation revealed more details about the various spinal bony lesions. Thus, it is concluded that computed tomography was non-invasive, highly sensitive imaging technique in diagnosing spinal injuries of dogs than conventional radiography.

KEYWORDS: Spinal injuries, Fracture, Computed tomography, Dogs, Radiography

Received 16 July, 2022; Revised 28 July, 2022; Accepted 31 July, 2022 © The author(s) 2022.

Published with open access at www.questjournals.org

I. INTRODUCTION

Most of the spinal diseases encountered frequently in small animal practice are usually associated with some neurologic dysfunctions which results in a various degrees of clinical signs like paresis and plegia. The thoracolumbar junction is the most common site of spinal injuries as it lies between the relatively rigid thoracic and more flexible lumbar spine (Thanigaivel *et al.*, 2017). Survey radiography and myelography are the first approach as well as the most commonly used method for the diagnosis of spinal diseases in veterinary practice. However, majority of the clinical cases in dogs showing longstanding neurological symptoms have no apparent abnormalities on survey radiography and there is a huge lacuna in diagnosing the spinal lesions, but the prognosis and treatment of spinal diseases are strongly relying on the degree of neurologic injury and its accurate assessment.

Computed tomography (CT) has been used widely as a as a first line approach diagnostic imaging modality of choice for neurological, oncological and orthopaedic cases in human medicine (Kinns *et al.*, 2006). Nowadays, in India, CT is now emerging as an important diagnostic technique especially in orthopaedic cases of animals. CT images has more advantage over conventional radiographs that, in former the image is depicted without the effects of superimposition and has superior soft tissue differentiation (contrast resolution) as well as the spatial resolution is also far superior. Hence, it also necessitates a step forward to CT application in veterinary medicine to make better diagnosis of spinal injuries. CT is also an efficient, sensitive, non-invasive diagnostic tool in imaging spinal injuries in veterinary practice especially in canine practice. Thus, the current study has been planned to compare and evaluate the radiographic and computed tomographic findings of traumatic spinal lesions in dogs.

II. MATERIALS AND METHODS

Six dogs presented to small animal surgery unit, Veterinary Clinical Complex, Namakkal, Tamil Nadu with spinal disorder were included in this study, irrespective of breed, age and sex. Neurological examination and grading of lesions on spinal segments were performed according to Palus 2014 and Denny and Butterworth 2000, respectively. Based on neurological examination severity of the spinal cord injury were graded from 1 to 7 (Denny and Butterworth, 2000).

Grade 1: Pain only

Grade 2: Ambulatory paraparesis / quadriparesis

Grade 3: Non-ambulatory paraparesis / quadriparesis

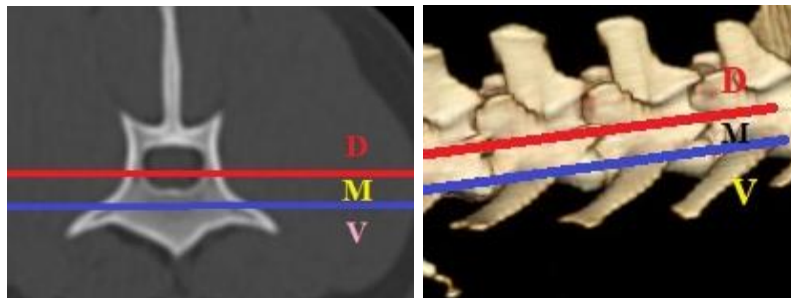
Grade 4: Paraplegia/quadriplegia

Grade 5: Paraplegia/quadriplegia + urinary retention with overflow (URO)

Grade 6: Paraplegia/quadriplegia + URO + loss of conscious pain sensation (CPS)

Grade 7: Ascending/descending myelomalacia

All the dogs were sedated with dexmedetomidine at a dose rate of 5µmg/kg body weight and butorphanol 0.2mg/kg body weight intravenously before subjecting to imaging procedure. Lateral and ventrodorsal radiograph of the spine were taken as localized by neurological evaluation. CT was performed using 16 slice CT unit (Toshiba). Lateral and ventrodorsal scout images were acquired prior to acquisition of transverse images. CT settings were 120 kV, 70 mAs, with a scan speed of 0.75 per rotation. Based on the radiographic findings of spine lesion transverse images were acquired at 3 mm slice thickness followed by slice thickness of 1 mm has been set especially for detailed post processing evaluation. 3D image is most flexible visualization tool, it benefits when presenting information to clients. Lesions are much easier for layperson to understand when visualized in this method and planning of fracture repair can be improved by 3D visualization of the injury (Schwarz *et al.*, 2000). When evaluating the transverse CT image, the degree of attenuation of spine was measured in Hounsfield units (HU) in cases suspected with disc mineralization and spondylosis. In order to do this region of interest (ROI) was chosen that was slightly smaller than the cross-sectional area. Stability of traumatic spinal injuries were assessed according to three column spine principle (Ricciardi 2016) Figure 1.



Three column spine principle for assessing stability of traumatic injuries
Figure 1: Evaluation of the stability of traumatic spinal injuries

III. RESULTS AND DISCUSSION

Neurological examination

Five dogs showed the signs of upper motor neuron (UMN) deficit by having lesions in T₃ to L₃ segment and one dog showed both upper and lower motor neuron (LMN) deficit while locating lesion in T₃ to L₃ and L₄ to S₂ segments respectively. Present study showed that dogs having lesions at L₄-S₂ (LMN dysfunction) have reduced or no spinal reflexes with spastic paraparesis whereas dogs with T₃-L₃ lesions (UMN dysfunction) also causes paraparesis with reduced proprioception with normal or exaggerated spinal reflexes. (Denny and Butterworth, 2000; Palus, 2014).

In this study, the dogs showed pain only, ambulatory paraparesis, non-ambulatory paraparesis, paraplegia/quadriplegia along with urinary retention with overflow (URO) and paraplegia/quadriplegia, URO with loss of conscious pain sensation (CPS) were graded as 1, 2, 3, 5 and 6 respectively. The grading of spinal lesions could be well correlated with gait abnormalities and results of spinal reflexes examination. These observations are concurred with the findings of Denny and Butterworth (2000).

Radiographic and computed tomographic examination

Case 1: Survey radiograph revealed vertebral body compression fracture at level of L₂ and complete vertebral body fracture at the level L₇ with cranioventral displacement of caudal portions. CT images revealed axial compression fracture at L₂ level and comminuted fracture vertebral body fracture with displacements of

fragments in the vertebral canal. Fracture was noticed in ventral and middle compartments at the level of L₂ and L₇ considered as unstable fracture. Figure 2.

Case 2: Plain radiography tentatively helped to diagnose one intervertebral disc prolapse based on narrowed intervertebral space between T₁₁ and T₁₂ whereas transverse plane between T₁₁₋₁₂ of CT revealed hyperdense area with density of $+161 \pm 50.9$ HU indicates the traumatic intervertebral disc extrusion. Figure 3.

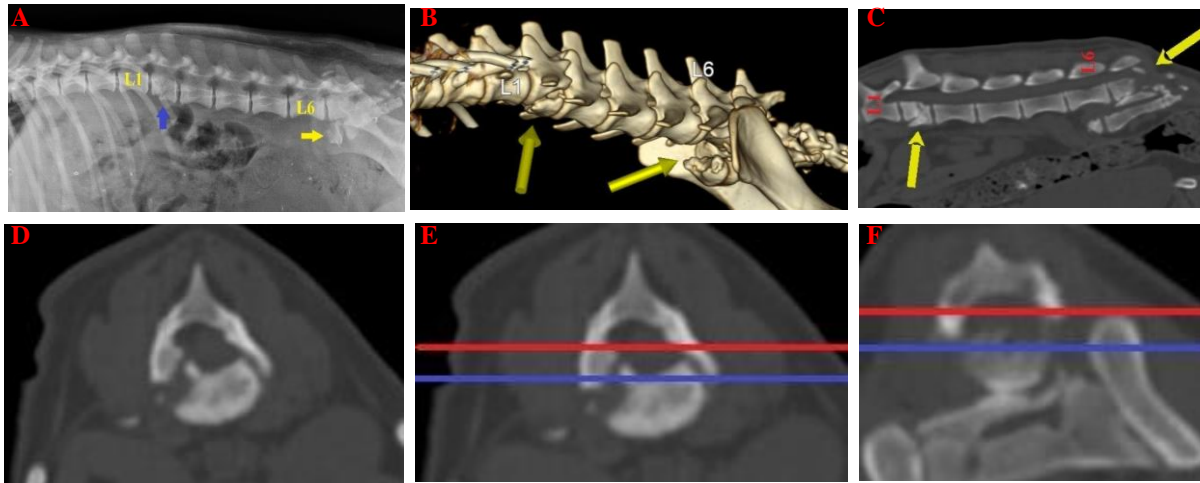


Figure 2 **A)** Lateral radiograph showing compression fracture at L₂ and fracture cum dislocation of L₇; **B)** 3D image showing fracture at the level of L₂ and L₇; **C)** Sagittal plane of lumbar region showing compression fracture at the level of L₂ and comminuted fracture with fragments displacement in vertebral canal at level of L₇; **D)** Transverse plane image at the level of L₂ showing fracture at the base of pedicle with luxation of vertebral body towards right side; **E** and **F)** Unstable fracture (Fracture was seen in middle and ventral compartments at the level L₂ and L₇)

Case 3: Periosteal new bone formation of the ventral and lateral margins was observed from T₈ to T₁₀ on plain



Figure 3 **A)** Lateral radiograph showing intervertebral compression of T₁₁ and T₁₂; **B)** Sagittal plane of thoracolumbar region revealed no space between T₁₁ and T₁₂ vertebral body; **C)** Transverse plane of T₁₁ and T₁₂ junction showing hyper dense area.

radiography, whereas CT revealed hypoattenuation of vertebral end plates from T₈ to T₁₀. Figure 4. Transverse CT image was useful in evaluating the migration of osteophytes into the spinal canal and cord compression. Spondylosis was observed in vertebrae other than the primary lesion segment which caused the neurological deficit. In some cases, even though the spondylosis was observed, it was not a sole etiology for neurological signs because invasion of ventral osteophyte into the spinal canal and spinal nerve compression was not possible whereas spondylosis with disc herniation was possible for nerve root compression. These findings were concurred with the observations of Akeda *et al.* (2015).

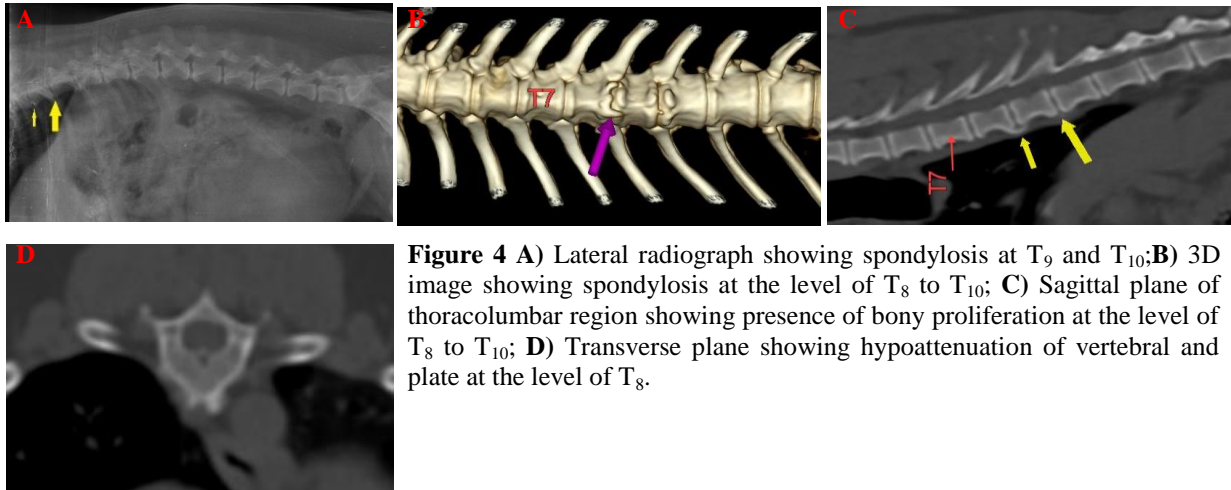


Figure 4 A) Lateral radiograph showing spondylosis at T₉ and T₁₀; B) 3D image showing spondylosis at the level of T₈ to T₁₀; C) Sagittal plane of thoracolumbar region showing presence of bony proliferation at the level of T₈ to T₁₀; D) Transverse plane showing hypoattenuation of vertebral and plate at the level of T₈.

Case 4: Lateral radiography revealed excessive mineralization of intervertebral disc and narrowing of both intervertebral space and foramen between L₁ to L₂. CT revealed multiple hyperattenuating mass was seen in between the intervertebral body of T₂₋₃, T₇₋₈, T₁₀₋₁₁ and L₁₋₂ on transverse plane, while at the same time transverse section of L₁₋₂ revealed the round focus of hyperattenuating material in the floor of the vertebral canal indicative of severe spinal compression with density of $+1086.7 \pm 293.4$ HU Figure 5. In present study, herniation of mineralized disc material into the vertebral canal was apparent even without the injection of subarachnoid contrast medium. CT density of the spinal cord was $+32.9 \pm 15.9$ HU whereas the CT density of the herniated disc was $+1086.7 \pm 293.4$ HU in soft tissue window. Hence, hyper attenuation variation could be helpful in diagnosing disc herniation (Olby *et al.* 2000; Lim *et al.*, 2010).

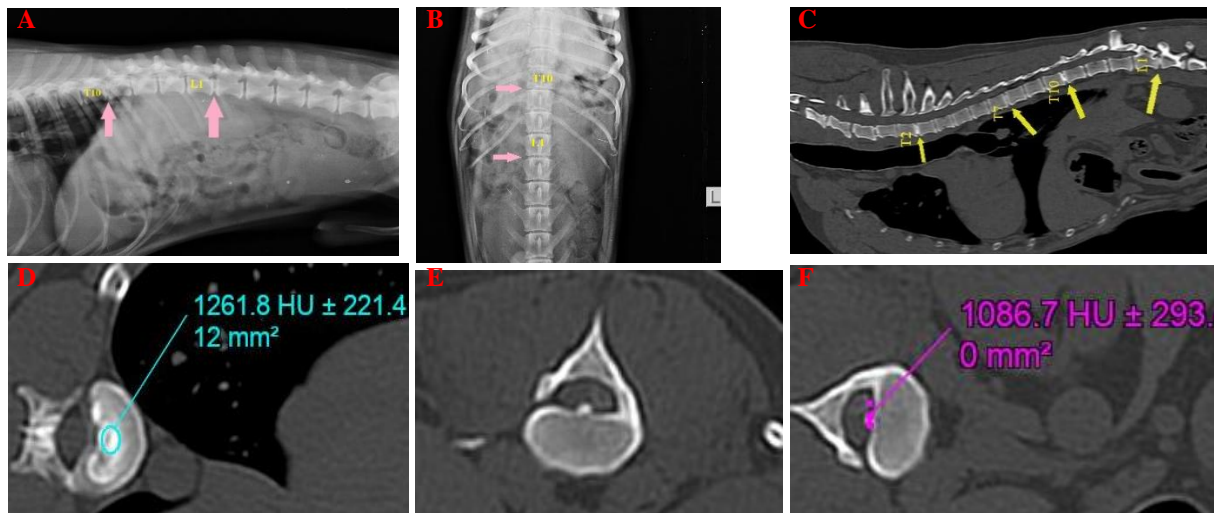


Figure 5 A and B) Lateral and ventrodorsal radiograph showing disc mineralization between T₁₀, T₁₁ and L₁, L₂ intervertebral space; C) Sagittal plane of thoraco-lumbar region showing disc mineralization at level of T₂₋₃, T₇₋₈, T₁₀₋₁₁ and L₁₋₂; D) Hyperattenuating material at level of T₁₀ intervertebral space; E and F) Transverse plane of L₁ showing round focus of hyperattenuating material in the floor of the vertebral canal, compressing the spinal cord.

Case 5: Thoracic spinal radiograph revealed fracture at caudal physis of T₁₁. CT sagittal view of thoraco-lumbar region revealed fracture of the caudal vertebral body physis suggesting Slatter Harris type I fracture at T₁₁ with concurrent ventral displacement of T₁₂. Transverse view of T₁₁ revealed fracture of spinous process, laminae, pedicles and ventral displacement of physeal fracture fragments as it involving in all three compartments considered as unstable Figure 6.

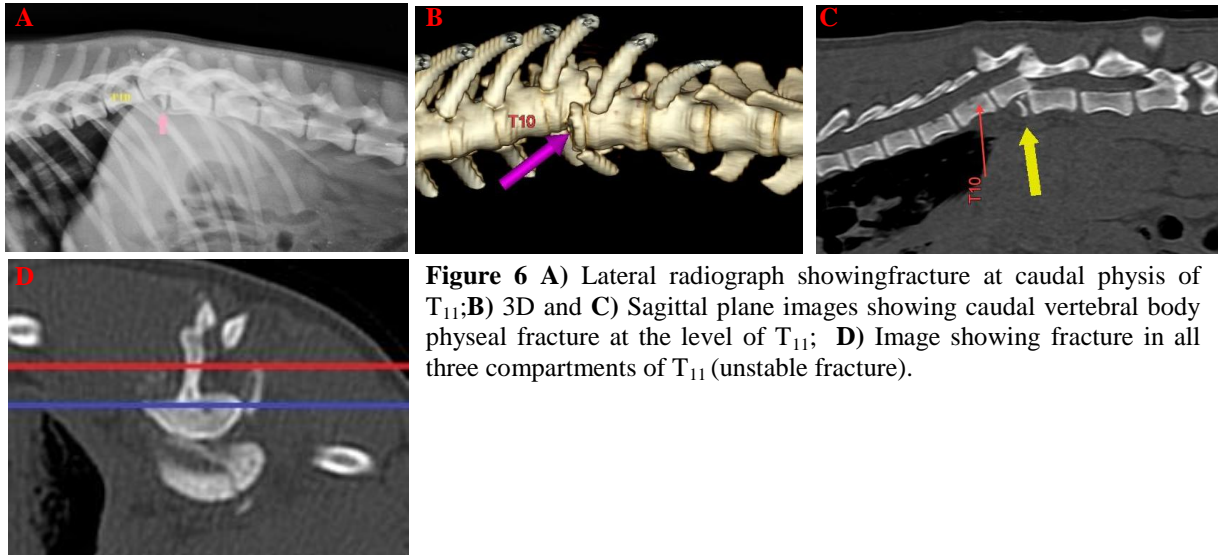


Figure 6 A) Lateral radiograph showing fracture at caudal physis of T₁₁; B) 3D and C) Sagittal plane images showing caudal vertebral body physal fracture at the level of T₁₁; D) Image showing fracture in all three compartments of T₁₁ (unstable fracture).

Case 6: The thoraco-lumbar spinal radiograph revealed oblique fracture of vertebral body at the level of L₁. CT sagittal section of thoraco-lumbar region revealed burst fracture with displacement of bone fragment in vertebral canal at the level of L₁ whereas the transverse section revealed multi fragmented burst fracture with displacement of bony fragments in vertebral canal of L₁. Further, 3D volume rendering of left thoraco-lumbar view revealed L₁ burst fracture, L₁ and L₂ left transverse process fracture along with dislocation of left T₁₃ rib. Figure 7.

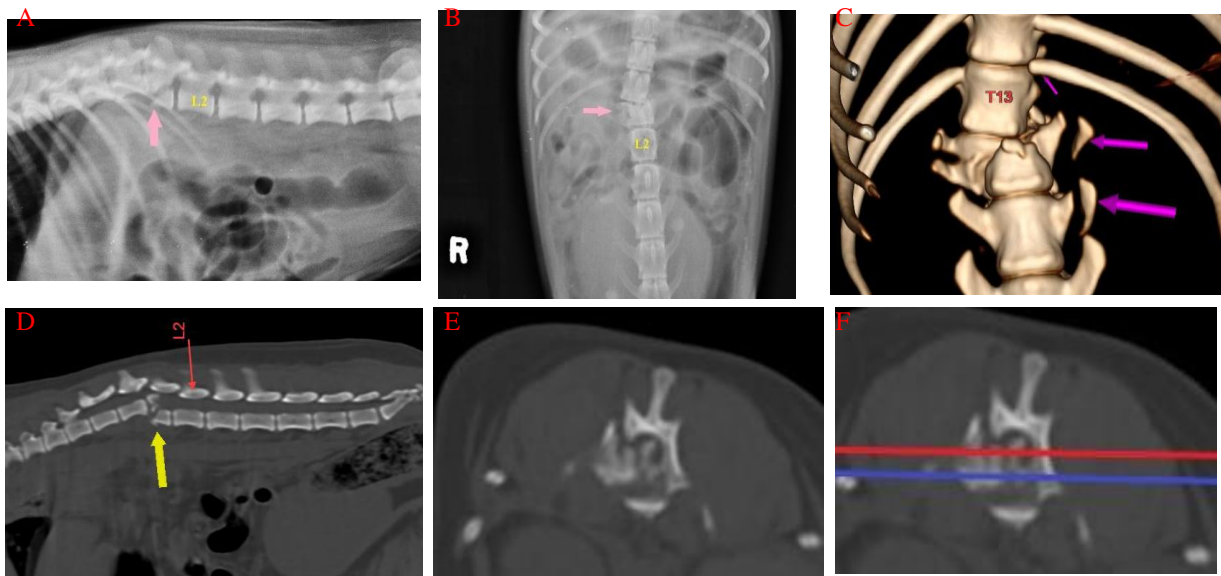


Figure 7 A and B) Lateral radiograph showing oblique fracture of L₁₁, respectively; C) 3D image showing L₁ vertebral body fracture, L₁ and L₂ left transverse process fracture along with dislocation of T₁₃ rib; D) Sagittal plane of thoracolumbar region showing L1 burst fracture with displacement of bone fragment in vertebral canal; E) Transverse plane of L1 showing burst fracture with displacement of bony fragments in vertebral canal; F) Image showing fracture in all three compartments of L₁.

In the present study, thoracolumbar spine was found to be the common site for fracture in all the cases, which could be attributed due to its location between the rigid thoracic spine and the well-muscled lumbar spine (Ricciardi, 2016; Bagley, 2000). Among the six cases, four are found to be associated with road traffic accident leads to various types fracture like compression, Slatter Harris type-I, burst fracture and traumatic intervertebral disc extrusion.

Fracture was seen in ventral compartment, middle and all three compartments in cases 1,6 and 5, respectively and stability of the fracture was assessed according to the three-column spine principle. Vertebral column was divided into three compartments: the dorsal compartment includes the spinous process, vertebral laminae, articular processes, vertebral pedicles and dorsal ligamentous complex (supraspinous ligament, interspinous ligament, joint capsule, ligamentum flavum). The middle compartment includes the dorsal longitudinal ligament, dorsal annulus fibrosus and dorsal vertebral body. The ventral compartment includes the remaining vertebral body, lateral and ventral aspects of annulus fibrosus, the nucleous pulposus and the ventral longitudinal ligament. Regardless of the degree of displacement of fracture, damage in two or more components were considered as unstable and suggested for surgical stabilization. This is in accordance with Kinns *et al.* (2006) and Ricciardi (2016).

Thus, it can be concluded that survey radiograph which is the first line of approach for diagnosis of spinal injuries in dogs, provided the anatomical land mark for major lesion with only limited details about the spinal injuries. The 2D nature of the radiograph along with superimposition by unrelated structure made it too difficult to visualize minute details of spinal injuries. CT endowed with contrast resolution with tomographic nature of prevented problem of superimposition, normally seen in typical radiograph. Thus, it makes CT, an ideal diagnostic technique for the characterization and localization of traumatic lesions affecting bones together with complex structure such as vertebrae, associated with position of fragments in relation to the spinal canal.

REFERENCES

- [1]. Akeda, K., T. Yamada, N. Inoue, A. Nishimura and A. Sudo. (2015). Risk factor for lumbar intervertebral disc height narrowing: a population- based longitudinal study in the elderly. *BMC Musculoskeletal Disorders*, **16**: 344.
- [2]. Bagley, R.S. (2000). Spinal fracture or luxation. *Vet. Clin. North Am. Small Anim. Pract.*, **30**: 133-153.
- [3]. Denny, H.R and S.J. Butterworth. (2000). A guide to canine and feline orthopaedic surgery. Fourth edition. Blackwell sciences Ltd. Chapter-17: 175-182.
- [4]. Kinns, J., W. Mai, Seiler., A. Zwingenberger and T. Schwarz. (2006). Radiographic sensitivity and negative predictive value for acute canine spinal trauma. *Vet Radiol Ultrasound*. **47**: 563-570.
- [5]. Lim, C., O. K. Kweon, M. C. Choi, J. Choi and J.Yoon. (2010). Computed tomographic characteristics of acute thoracolumbar intervertebral disc disease in dogs. *J. Vet. Sci*, **11**(1): 73-79.
- [6]. Olby, N.J., K.R. Müntana, N.J. Sharp, and D.E. Thrall. (2000). The computed tomographic appearance of acute thoracolumbar intervertebral disc herniations in dogs. *Vet Radiol Ultrasound*, **41**(5): 396-402.
- [7]. Palus, V. (2014). Neurological examination in small animals. *Macedonian Veterinary Review*, **37**(1): 95-105.
- [8]. Ricciardi, M. (2016). Usefulness of multidetector computed tomography in the evaluation of spinal neuro-musculoskeletal injuries. *Veterinary and Comparative Orthopaedics and Traumatology*, **29**(01): 1-13.
- [9]. Schwarz, T., M.R. Owen, S. Long and M. Sullivan. (2000). Vacuum disc and facet phenomenon in a dog with cauda equine syndrome. *Jam Vet Med Assoc*, **217**(6):862-864.
- [10]. Thanigaivel, P., S. Ayyapan, R. Jayaprakash, S. Balasubramanian and M. Thamizhannal. (2017). Evaluation of Radiological Findings of Dogs with Thoracolumbar Disorders. *Int. J. Environ. Sci. Technol.*, **6**(1):191-198.